

CHAPTER 2 MODELING OF SLOSHING

*remember, when discoursing about water,
to induce first experience, then reason.
- Leonardo Da Vinci*

In this chapter, modeling of liquid sloshing in TLDs is presented. The first approach is aimed at understanding the underlying physics of the problem based on a “Sloshing-Slamming (S^2)” analogy which describes the behavior of the TLD as a linear sloshing model augmented with an impact subsystem. The second model utilizes certain nonlinear functions known as impact characteristic functions, which clearly describe the nonlinear behavior of TLDs in the form of a mechanical model. The models are supported by numerical simulations which highlight the nonlinear characteristics of TLDs.

2.1 Introduction

The motion of liquids in rigid containers has been the subject of many studies in the past few decades because of its frequent application in several engineering disciplines. The need for accurate evaluation of the sloshing loads is required for aerospace vehicles where violent motions of the liquid fuel in the tanks can affect the structure adversely (Graham and Rodriguez, 1952; Abramson, 1966). Liquid sloshing in tanks has also received considerable attention in transportation engineering (Bauer, 1972). This is important for problems relating to safety, including tank trucks on highways and liquid tank cars on railroads. In maritime applications, the effect of sloshing of liquids present on board,

e.g., liquid cargo or liquid fuel, can cause loss of stability of the ship as well as structural damage (Bass *et al.* 1980). In structural applications, the effects of earthquake induced loads on storage tanks need to be evaluated for design (Ibrahim *et al.* 1988). Recently however, the popularity of TLDs as viable devices for structural control has prompted study of sloshing for structural applications (Modi and Welt 1987; Kareem and Sun 1987; Fujino *et al.* 1988).

2.1.1 Numerical Modeling of TLDs

The first approach in the modeling of sloshing liquids involves using numerical schemes based on linear and/or non-linear potential flow theory. These type of models represent extensions of the classical theories by Airy and Boussinesq for shallow water tanks. Faltinson (1978) introduced a fictitious term to artificially include the effect of viscous dissipation. For large motion amplitudes, additional studies have been conducted by Lepelletier and Raichlen (1988); Okamoto and Kawahara (1990); Chen *et al.* (1996) among others. Numerical simulation of sloshing waves in a 3-D tank has been conducted by Wu *et al.* (1998).

The model presented by Lepelletier and Raichlen (1988) recognized the fact that a rational approximation of viscous liquid damping has to be introduced in order to model sloshing at higher amplitudes. Following this approach, a semi-analytical model was presented by Sun and Fujino (1994) to account for wave breaking in which the linear model was modified to account for breaking waves. Two experimentally derived empirical constants were included to account for the increase in liquid damping due to breaking waves and the changes in sloshing frequency, respectively. The attenuation of the waves in the mathematical model due to the presence of dissipation devices is also possible through a

combination of experimentally derived drag coefficients of screens to be used in a numerical model (Hsieh *et al.* 1988). Additional models of liquid sloshing in the presence of flow dampening devices are reported, e.g., Warnitchai and Pinkaew (1998). The main disadvantage of such numerical models is the intensive computational time needed to solve the system of finite difference equations.

Numerical techniques for modeling sloshing fail to capture the nonlinear behavior of TLDs. This is due to the inability of theoretical models to achieve long time simulations due to numerical loss of fluid mass (Faltinsen and Rognebakke, 1999). Moreover, it is very difficult to incorporate slamming impact in a direct numerical method. Accurate predictions of impact pressures over the walls of the tanks requires the introduction of local physical compressibility in the governing equations. The rapid change in time and space require special treatment which is currently unavailable in existing literature. However, recent work in numerical simulation of violent sloshing flows in deep water tanks are encouraging and represent the state-of-the-art in this area, e.g, Kim (2001). However, until the numerical schemes are more developed, one has to resort to mechanical models for predicting the sloshing behavior. The chief advantages of a mechanical model are savings in computational time and a good basis for design of TLDs.

2.1.2 Mechanical Modeling of TLDs

For convenient implementation in design practice, a better model for liquid sloshing would be to represent it using a mechanical model. This is helpful in combining a TLD system with a given structural system and analyzing the overall system dynamics. Some of the earliest works in this regard are presented in Abramson (1966). Most of these are linear models based on the potential formulation of the velocity field. For shallow water

TLDs, various mechanisms associated with the free liquid surface come into play to cause energy dissipation. These include hydraulic jumps, bores, breaking waves, turbulence and impact on the walls (Lou *et al.* 1980). The linear models fail to address the effects of such phenomena on the behavior of the TLD.

Sun *et al.* (1995) presented a tuned mass damper analogy for non-linear sloshing TLDs. The interface force between the damper and the structure was represented as a force induced by a virtual mass and dashpot. The analytical values for the equivalent mass, frequency and damping were derived from a series of experiments. The data was curve-fitted and the resulting quality of the fit was mixed due to the effects of higher harmonics. Other non-linear models have been formulated as an equivalent mass damper system with non-linear stiffness and damping (e.g., Yu *et al.* 1999). These models can compensate for the increase in sloshing frequency with the increase in amplitude of excitation. This hardening effect is derived from experimental data in terms of a stiffness hardening ratio. However, none of these models explain the physics behind the sloshing phenomenon at high amplitudes.

In contrast with the preceding models, Yalla and Kareem (1999) presented an analogy which attempts to explain the metamorphosis of linear sloshing to a nonlinear hardening sloshing system and the observed increase in the damping currently not fully accounted for by the empirical correction for wave breaking. At high amplitudes, the sloshing phenomenon resembles a rolling convective liquid mass slamming/impacting on the container walls periodically. This is similar to the impact of breaking waves on bulkheads observed in ocean engineering. None of the existing numerical and mechanical

models for TLDs account for this impact effect on the walls of the container. The sloshing-slamming (S^2) is described in detail in the following section.

2.2 Sloshing-Slamming (S^2) Damper Analogy

The sloshing-slamming (S^2) analogy is a combination of two types of models: the linear sloshing model and the impact damper model.

2.2.1 Liquid Sloshing

A simplified model of sloshing in rectangular tanks is based on an equivalent mechanical analogy using lumped masses, springs and dashpots to describe liquid sloshing. The lumped parameters are determined from the linear wave theory (Abramson, 1966). The equivalent mechanical model is shown schematically in Fig. 2.1(a). The two key parameters are given by:

$$m_n = M_l \left(\frac{8 \tanh \{ (2n-1)\pi r \}}{\pi^3 r (2n-1)^3} \right); \quad n=1, 2, \dots \quad (2.1)$$

$$\omega_n^2 = \frac{g(2n-1)\pi \tanh \{ (2n-1)\pi r \}}{a}; \quad n=1, 2, \dots \quad (2.2)$$

where n is the sloshing mode; m_n is the mass of liquid acting in that mode; ω_n is the frequency of sloshing; $r = h/a$ where h is the height of water in the tank; a is the length of the tank in the direction of excitation; M_l is the total mass of the water in the tank; and m_o is

the *inactive mass* which does not participate in sloshing, given by $m_o = M_l - \sum_{n=1}^{\infty} m_n$.

Usually, only the fundamental mode of liquid sloshing (i.e., $n = 1$) is used for analysis. This model works well for small amplitude excitations, where the wave breaking and

the influence of non-linearities do not influence the overall system response significantly. This model can also be used for initial design calculations of TLDs (Tokarczyk, 1997).

2.2.2 Liquid Slamming

An analogy between the slamming of liquid on the container walls and an impact damper is proposed. An impact damper is characterized by the motion of a small rigid mass placed in a container firmly attached to the primary system, as shown in Fig. 2.1(b) (e.g., Masri and Caughey, 1966; Semercigil *et al.* 1992; Babitsky, 1998). A gap between the container and the impact damper, denoted by d , is kept by design so that collisions take place intermittently as soon as the displacement of the primary system exceeds this clearance. The collision produces energy dissipation and an exchange of momentum. The primary source of attenuation of motion in the primary system is due to this exchange of momentum. This momentum exchange reverses the direction of motion of the impacting mass. The equations of motion between successive impacts are given by

$$M\ddot{x} + C\dot{x} + Kx = F_e(t) \quad (2.3)$$

$$m\ddot{z} = 0 \quad (2.4)$$

The velocity of the primary system after collision is given as (Masri and Caughey, 1966)

$$\dot{x}_{ac} = \frac{(1 - \mu e)}{(1 + \mu)} \dot{x}_{bc} + \frac{\mu(1 + e)}{(1 + \mu)} \dot{z}_{bc} \quad (2.5)$$

where e is the coefficient of restitution of the materials involved in the collision, $\mu = m/M$ is the mass ratio, x and z represent the displacement of the primary and secondary system, and the subscripts ac and bc refer to the *after-collision* and *before-collision* state of the

variables. The velocity of the impact mass is reversed after each collision. The numerical simulation of this model is discussed in the next section.

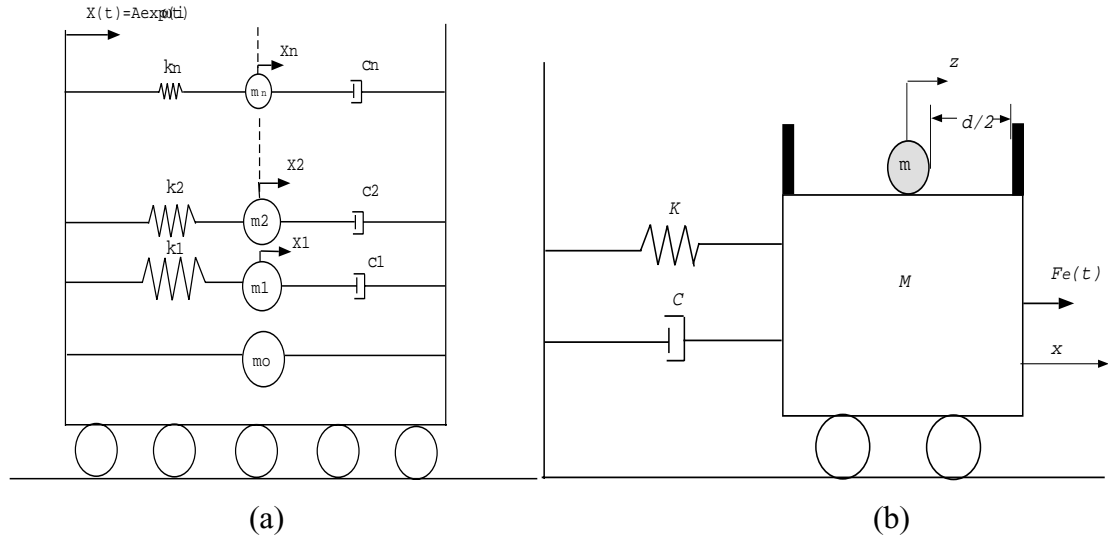


Figure 2.1 (a) Equivalent mechanical model of sloshing liquid in a tank (b) Impact damper model

2.2.3 Proposed Sloshing-Slamming (S^2) Analogy

The experimental work on the sloshing characteristics of TLDs has been reported by Fujino *et al.* (1992); Reed *et al.* (1998); Yu *et al.* (1999), etc. The key experimental results are summarized in Figs. 2.2 (a) and (b), where the jump frequency and the damping ratio are shown to increase with the amplitude of excitation. The jump phenomenon is typical of nonlinear systems in which the system response drops sharply beyond a certain frequency known as the jump frequency. These results have been taken from Yu *et al.* (1999) where the increase in damping and the change in frequency have been plotted as a function of non-dimensional amplitude given as A_e/a , where A_e is the amplitude of excitation and a is the length of the tank in the direction of excitation.

Figure 2.2 (a) shows that there is an increase in the jump frequency (κ) at higher amplitudes of excitation for the frequency ratios ($\gamma_f = \omega_e/\omega_f$) greater than 1 suggesting a hardening effect, where ω_e is the frequency of excitation and ω_f is the linear sloshing frequency of the damper. It has been noted that as the amplitude of excitation increases, the energy dissipation occurs over a broader range of frequencies. This feature points at the robustness of TLDs. The coupled TLD-structure system exhibits certain nonlinear characteristics as the amplitude of excitation increases. Experimental studies suggest that the frequency response of a TLD, unlike a TMD, is excitation amplitude dependent. The increased damping (introduced by wave breaking and slamming) causes the frequency response function to change from a double-peak to a single-peak function. This has been observed experimentally by researchers, e.g., Sun and Fujino, 1994.

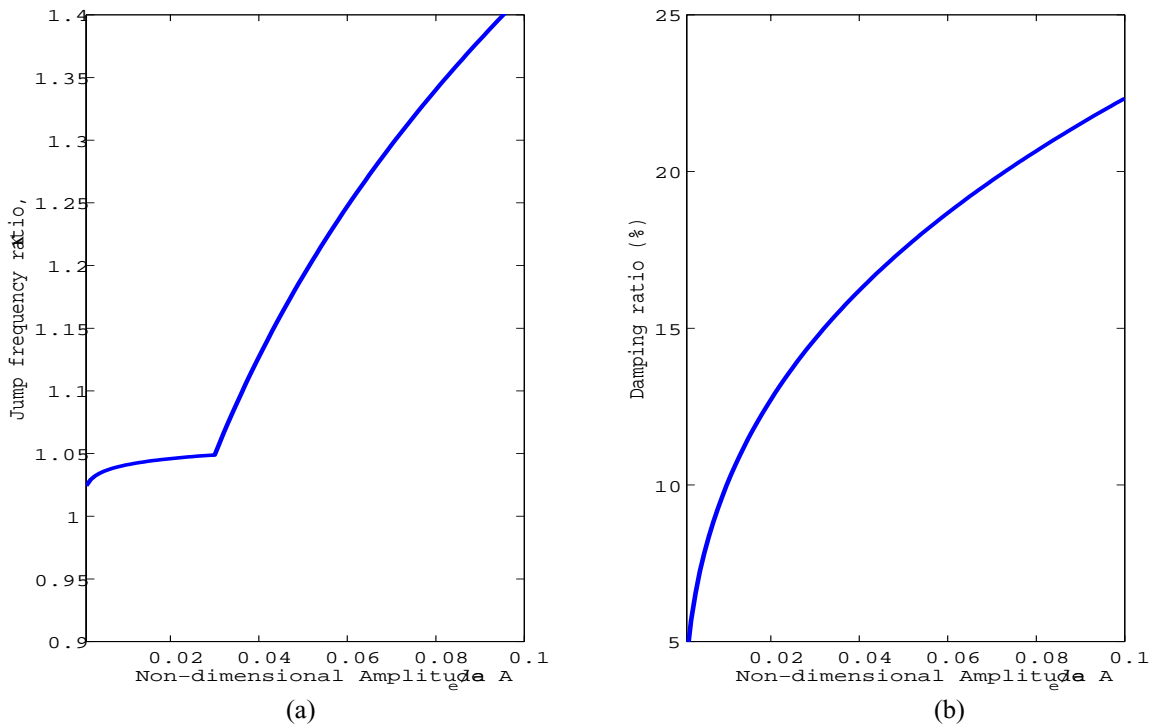


Figure 2.2 Variation of (a) jump frequency and (b) damping ratio of the TLD with the base amplitude (Yu et al. 1999).

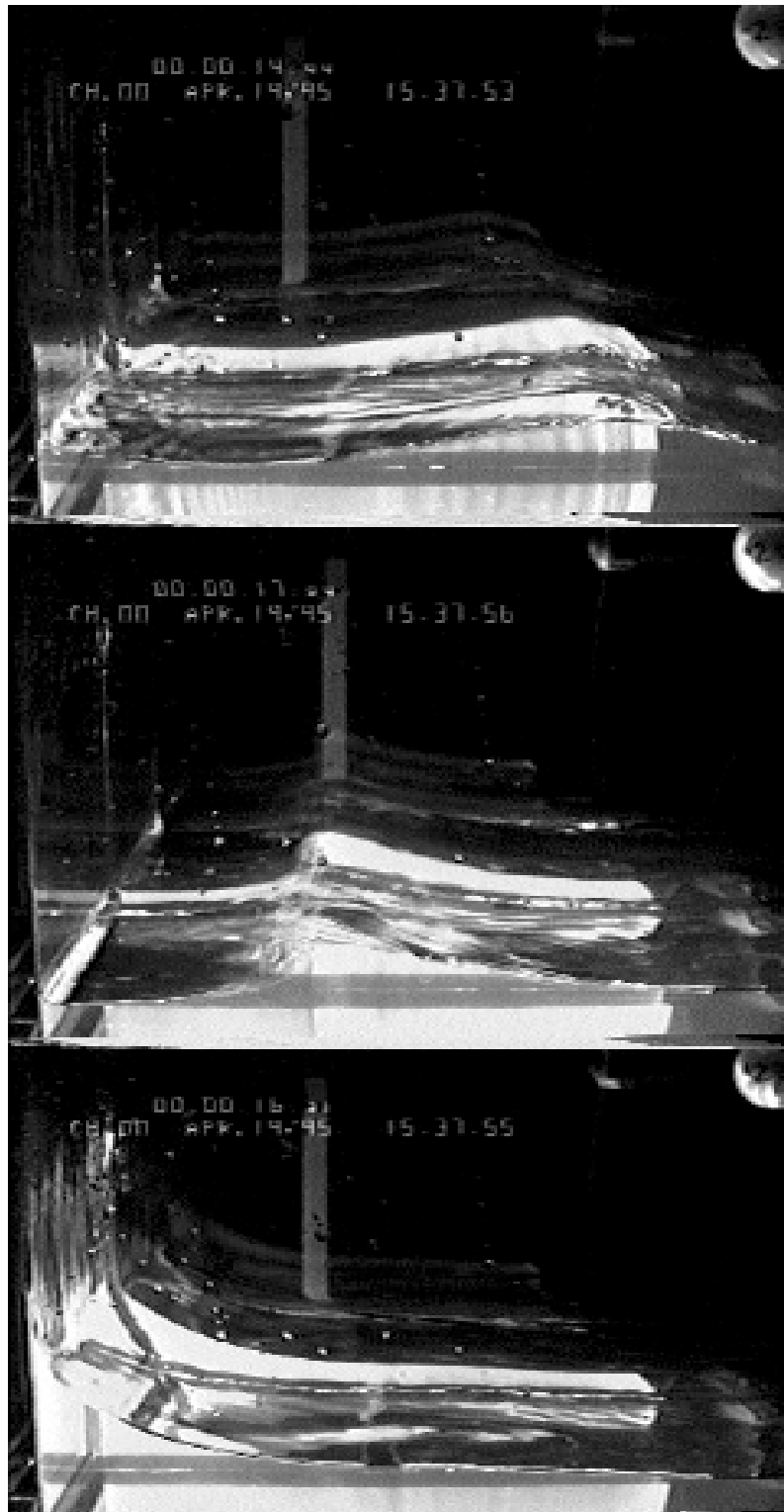


Figure 2.3 Frames from the sloshing experiments video at high amplitudes: a part of water moves as a lumped mass and impacts the container wall. (*Video Courtesy: Dr. D.A. Reed*)

SLOSHING-SLAMMING DAMPER ANALOGY

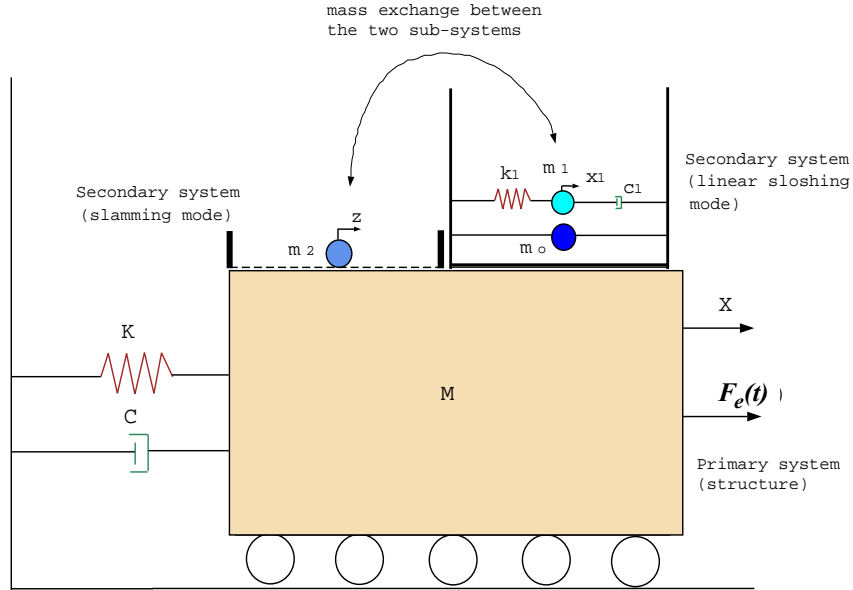


Figure 2.4 Schematic diagram of the proposed sloshing-slaming (S^2) analogy

As will be shown herein, the experimental observations that at higher amplitudes, the liquid motion is characterized by slamming/impacting of water mass (Fig. 2.3). This includes wave breaking and the periodic impact of convecting lumped mass on container walls. Some of the energy is also dissipated in upward deflection of liquid along the container walls. The S^2 damper analogy is illustrated schematically in Fig. 2.4. Central to this analogy is the exchange of mass between the sloshing and convective mass that impacts. This means that at higher amplitudes, some portion of the mass m_1 (the linear sloshing liquid), is exchanged to mass m_2 (the impact mass), which results in a combined sloshing-slaming action.

The level of mass exchange is related to the change in the jump frequency as shown in Fig. 2.2(a). A mass exchange parameter Ω is introduced, which is an indicator

of the portion of linear mass m_l acting in the linear mode. Since the total mass is conserved, this implies that the rest of the mass is acting in the impact mode. For example, $\Omega = 1.0$ means that all of the mass m_l is acting in the linear sloshing mode. After the mass exchange has taken place, the new masses \tilde{m}_1 and \tilde{m}_2 in the linear sloshing mode and the impact mode, respectively, are given by

$$\tilde{m}_2 = m_2 + (1 - \Omega)m_1 \quad (2.6)$$

$$\tilde{m}_1 = \Omega m_1 \quad (2.7)$$

At low amplitudes, there is almost no mass exchange, therefore, the linear theory holds. However, as the amplitude increases, γ decreases and the slamming mass increases concomitantly. Moreover, since m_l is decreasing, the sloshing frequency increases, which explains the hardening effect. The mass exchange parameter can be related to the jump

frequency ratio. Since $\omega_1^2 = \frac{k_1}{\tilde{m}_1} = \frac{\omega_1^2 m_1}{\tilde{m}_1}$, therefore using Eq. 2.7, one can obtain

$\kappa = \sqrt{1/\Omega}$. The empirical relations as shown in Fig. 2.2(a) for relating the mass exchange parameter to the amplitude of excitation can be introduced to the proposed scheme. This scheme can be further refined should it become possible to quantify more accurately the mass exchange between the sloshing and slamming modes from theoretical considerations. The equations of motion for the system shown in Fig. 2.4 can be written as

$$\begin{aligned} M\ddot{X} + (C + c_1)\dot{X} + (K + k_1)X - c_1\dot{x}_1 - k_1x_1 &= F_o \sin(\omega_e t) \\ m_1\ddot{x}_1 + c_1\dot{x}_1 + k_1x_1 - c_1\dot{X} - k_1X &= 0 \\ m_2\ddot{z} &= 0 \end{aligned} \quad (2.8)$$

where $F_o = MA_e \omega_e^2$. After each impact, the velocity of the convecting liquid is changed in accordance with Eq. 2.5. An impact is numerically simulated at the time when the relative displacement between m_1 and m_2 is within a prescribed error tolerance of $d/2$, i.e., $|x_1 - z| \pm \varepsilon = d/2$. In this study the error tolerance has been assumed as $\varepsilon/d = 10^{-6}$. Since the relative displacements have to be checked at each time step, a time domain integration scheme is employed to solve the system of equations. In order to construct the frequency response curves, the maximum steady-state response was observed at each excitation frequency and the entire procedure was repeated for the complete range of excitation frequencies.

2.2.4 Numerical Study

A numerical study was conducted using the parameters employed in the experimental study (Fujino *et al.* 1992). These parameters are listed in Table 2.1. It should be noted that the initial mass ratio, prior to the mass exchange, has been assumed to take on a very small value, i.e., $m_2/m_1 = 0.01$, which is essential to realize the system in Fig. 2.4 described by Eq. 2.8. This assumption is not unjustified since experimental results show the presence of nonlinearity in the transfer function, albeit small, even at low amplitudes of excitation (e.g., at $A_e = 0.1$ cm, $\kappa = 1.02$). Figure 2.5 shows the changes that take place in the frequency response functions as the mass exchange parameter is varied. This can also be viewed as the amplitude dependent variation in the frequency response function. It should be noted that the frequency response function undergoes a change from a double-peak to a single-peak function at higher amplitudes of excitation. This model gives similar results as Fujino *et al.* 1992, however, one has to note that this is a mechanical model as

opposed to a numerical model described in Fujino *et al.* 1992. These results demonstrate that the frequency response function of the combined system derived from the sloshing-slammng model is in good agreement with the experimental data both at low and high amplitudes of excitation. Note that uncontrolled and controlled cases in Fig. 2.5 refer to structure without and with TLD.

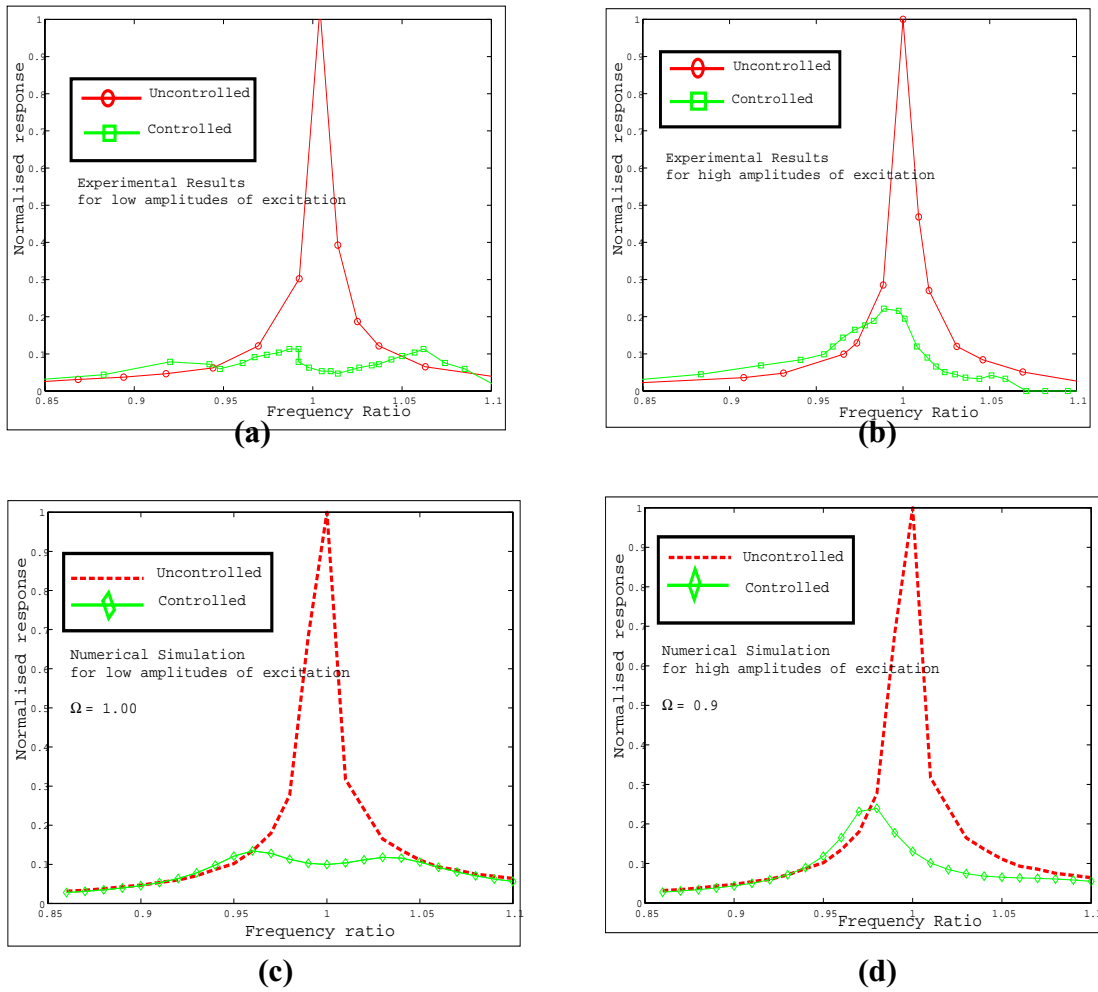


Figure 2.5 Comparison of experimental results with S^2 simulation results: (a), (b): experimental results (Fujino *et al.* 1992); (c), (d): simulation results for $\Omega = 1.0$ and $\Omega = 0.9$

TABLE 2.1 Parameters of the model

Parameter	value	Parameter	value
Main mass M	168 Kg	breadth of tank, b	32 cm
Main mass damping	0.32 %	height of water, h	2.1 cm
Natural freq. of main mass	5.636 rad/s	Coefficient of restitution, e	0.4
Length of tank, a	25 cm	Impact Clearance $d/(Fo/k)$	20
Mass ratio m_1/M	0.01	Initial mass ratio m_2/m_1	0.01

2.2.5 Base Shear Force

It has been said before that the sloshing exhibits the presence of the jump phenomenon as the amplitude of excitation increases. This jump phenomenon is typical of most nonlinear systems, for e.g., duffing, vanderpol oscillators, etc. A typical transfer function of a nonlinear system is shown in Fig. 2.6(a). The non-dimensionalized experimental base shear of TLD is plotted for various amplitudes of excitation in Fig 2.6(b) (Fujino *et al.* 1992). The presence of jump and hardening phenomenon can be clearly observed. Furthermore, the range of frequencies over which the TLD is effective increases as the base amplitude increases.

The S^2 damper analogy cannot be directly applied to the liquid damper alone due to the way it is formulated since to determine the post-impact velocity, one requires the knowledge of the dynamics of the primary system. Therefore, in order to formulate a single model which explains the experimental results for both damper characteristic and the coupled structure-damper system, one can take advantage of certain impact characteristics which describe the effects of nonlinearities imposed by the slamming mass. When repetitive impacts occur as part of the vibratory motion of a linear system, the problem becomes nonlinear. Having recognized this, one can search for such impact-characteristic functions

which would produce the same nonlinearities in the linear system. This is studied in the next section.

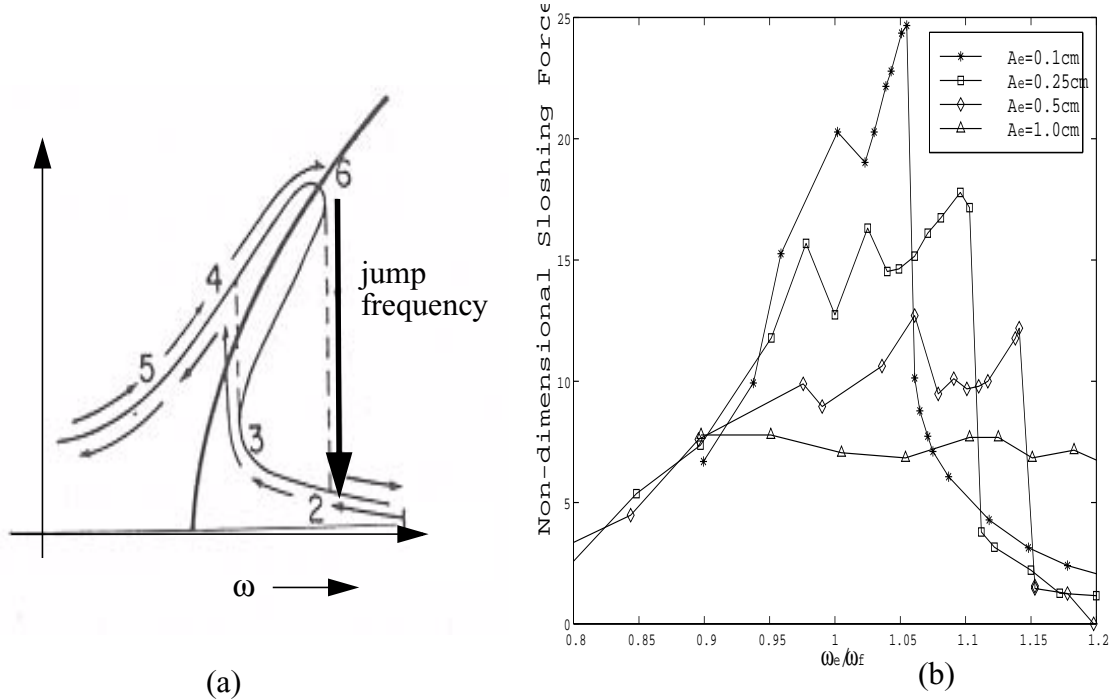


Figure 2.6 (a) Jump phenomenon in nonlinear systems (b) Variation of the non-dimensionalized base shear force with the frequency ratio (experimental results taken from Fujino et al. 1992).

2.3 Impact Characteristics model

In earlier section on sloshing-slaming damper analogy, the impact of the liquid on the container walls was simulated using the solution of differential equations, also known as the point-wise mapping method. The impact was modeled as a collision between the slamming (impact) mass and the tank wall as a discontinuous function. However, from the extensive work done in the area of vibro-impact systems, it is known that the dynamic model studied is a *limiting* case of a hardening type of nonlinear system not only in terms of structure but also function. It is well known in vibro-impact literature that one can

model the impact behavior by considering impact characteristics instead of simulating impacts by numerical integration schemes (Pilipchuk and Ibrahim, 1997; Babitsky, 1998). Hence, the basic character of the nonlinear behavior for vibro-impact systems obtained using “exact” methods are similar to typical nonlinear hardening systems. In fact, a very simple model can phenomenologically describe the interaction between the liquid mass and the tank wall with a nonlinear function. Having recognized this, one can search for such *impact characteristic* functions which would produce the same effect as the solution of differential equations. This equivalence was demonstrated for harmonic as well as random excitations (Masri and Caughey, 1965). It is to be noted that in this case, we will not distinguish the liquid mass into impact mass and sloshing mass as done in the previous section. The nonlinear model is developed for the entire liquid mass. Consider a oscillator model given as:

$$m\ddot{x} + c\dot{x} + kx + m\Phi(x, \dot{x}) = F_o \sin(\omega_e t) \quad (2.9)$$

where $\Phi(x, \dot{x})$ are the impact characteristics of the system, x is the displacement of the lumped mass; \dot{x} is the velocity of the lumped mass; m , c and k are the mass, damping and stiffness terms of the oscillator; F_o is the excitation amplitude = $m\omega_e^2 A_e$. One can assume the impact characteristics as a combination of different nonlinear functions of the displacement and velocity. In particular, Hunt and Crossley (1975) presented nonlinear impact characteristics whereby one can interpret the coefficient of restitution as damping in vibro-impact. They suggest the following form of the impact system:

$$\Phi(x, \dot{x}) = b_1 x^{P_1} \dot{x} + b_2 x^{P_2} \quad (2.10)$$

where b_1 , b_2 , p_1 and p_2 are parameters of the model. However, for the sake of keeping the model simple, we assume the impact characteristics to be dependent on the displacement, i.e., $\Phi(x, \dot{x}) = \Phi(x)$, while maintaining the damping to be a nonlinear function of the amplitude of excitation. Accordingly Eq. 2.9 can be expressed in the following non-dimensional form as:

$$\ddot{x} + 2\omega_f \zeta(A_e) \dot{x} + \Phi(x) = \omega_e^2 A_e \sin(\omega_e t) \quad (2.11)$$

where ω_f is the linear sloshing frequency and $\zeta(A_e)$ is the nonlinear damping of the TLD. In this study, we will focus exclusively on shallow water TLDs, i.e. $h/a < 0.15$, where h = depth of water and a = length of the tank in the direction of the excitation.

Various functions were considered for modeling the impact characteristics, e.g., hyperbolic sine function, power law function, and bi-linear hardening type function. Figure 2.7 shows the power law function used for modeling the impact characteristics. The power law curve is used in this study since it allows for a finite value of the impact characteristic function at the boundaries of the wall, i.e., $x = \pm a/2$. Note that the ordinate is the non-dimensionalized displacement of the liquid sloshing mass.

The interaction force is written as a function of displacement of the sloshing mass:

$$F_{eff}(x) = F_{lin} + F_{non-lin} \quad (2.12)$$

$$F_{eff}(x) = k_{eff}(x)x = m\omega_f^2 [1 + \varphi(A_e)x^{2(\eta-1)}]x \quad (2.13)$$

where $\varphi(A_e)$ and η are the parameters of the impact characteristic function $\Phi(x)$.

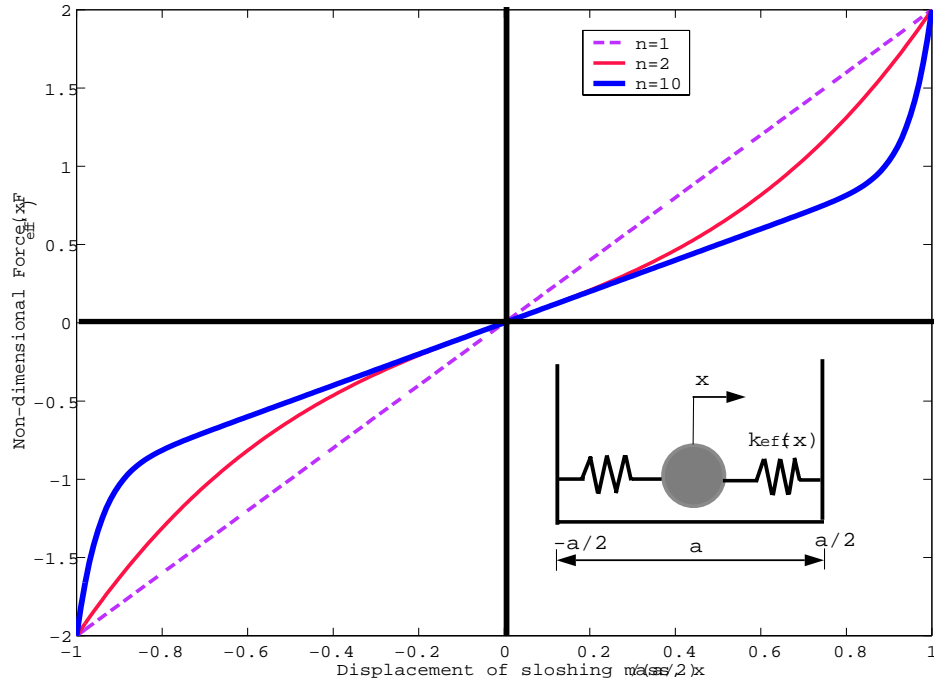


Figure 2.7 Non dimensional interaction force curves for different η

2.4 Equivalent Linear Models

Equivalent linear models are useful for initial approximation of the periodic solution of nonlinear systems. Moreover, one can represent these systems in transfer function or state-space form to simplify the analysis by utilizing the linear systems theory. In the next sub-sections we will briefly look at equivalent linear models when the external excitation is harmonic and random.

2.4.1 Harmonic Linearization

The nonlinear impact characteristics can be linearized as,

$$\Phi(x, \dot{x}) = \lambda + \upsilon x + \psi \dot{x} \quad (2.14)$$

The basic idea is to first define an error function and minimize it in the mean square sense over an infinite time interval. One can write the error function as,

$$\Theta(\lambda, \nu, \psi) = \lim_{T \rightarrow \infty} \frac{1}{T} \int_0^T \{\Phi(x, \dot{x}) - \lambda - \nu x - \psi \dot{x}\}^2 dt \quad (2.15)$$

One can assume the solution of the form:

$$x(t) = a_x \cos(\omega t) \text{ and } \dot{x}(t) = -a_x \omega \sin(\omega t) \quad (2.16)$$

Utilizing the fact that $\frac{\partial}{\partial \lambda} \Theta(\lambda, \nu, \psi) = 0$; $\frac{\partial}{\partial \nu} \Theta(\lambda, \nu, \psi) = 0$ and $\frac{\partial}{\partial \psi} \Theta(\lambda, \nu, \psi) = 0$

and recognizing the following properties of the solution:

$$\lim_{T \rightarrow \infty} \frac{1}{T} \int_0^T x(t) dt = 0 ; \lim_{T \rightarrow \infty} \frac{1}{T} \int_0^T \dot{x}(t) dt = 0 \text{ and } \lim_{T \rightarrow \infty} \frac{1}{T} \int_0^T x(t) \dot{x}(t) dt = 0 \quad (2.17)$$

one can arrive at the following equations

$$\lambda = \lim_{T \rightarrow \infty} \frac{1}{T} \int_0^T \Phi(x, \dot{x}) dt \quad (2.18)$$

$$\nu = \frac{1}{\sigma_x^2} \lim_{T \rightarrow \infty} \frac{1}{T} \int_0^T \Phi(x, \dot{x}) x(t) dt \quad (2.19)$$

$$\psi = \frac{1}{\sigma_{\dot{x}}^2} \lim_{T \rightarrow \infty} \frac{1}{T} \int_0^T \Phi(x, \dot{x}) \dot{x}(t) dt \quad (2.20)$$

where $\sigma_x = a_x / \sqrt{2}$ and $\sigma_{\dot{x}} = (a_x \omega) / \sqrt{2}$ for harmonic motion.

2.4.2 Statistical Linearization

In this case also, one can define a error functional similar to Eq. 2.15 as:

$$\Theta(\lambda, \nu, \psi) \equiv E(\{\Phi(x, \dot{x}) - \lambda - \nu x - \psi \dot{x}\}^2) \quad (2.21)$$

where $E(g(x, \dot{x}))$ represents the expected value of the random variable function $g(x, \dot{x})$.

Using similar procedure as before and recognizing that $E(x\dot{x}) = 0$; $E(x^2) = \sigma_x^2$ and

$E(\dot{x}^2) = \sigma_{\dot{x}}^2$, one can obtain the following expressions:

$$\lambda = \int_{-\infty}^{\infty} \Phi(u)w(u)du \quad (2.22)$$

$$\nu = \frac{1}{\sigma_x^2} \int_{-\infty}^{\infty} u\Phi(u)w(u)du \quad (2.23)$$

$$\psi = \frac{1}{\sigma_{\dot{x}}^2} \int_{-\infty}^{\infty} \dot{u}\Phi(\dot{u})w(\dot{u})d\dot{u} \quad (2.24)$$

where it is assumed that x and \dot{x} are independent Gaussian processes with probability distribution function defined by,

$$w(u) = \frac{1}{\sigma_u \sqrt{2\pi}} \exp\left(\frac{-u^2}{2\sigma_u^2}\right) \quad (2.25)$$

and the nonlinear function can be represented in a separable form, i.e.,

$$\Phi(x, \dot{x}) = \Phi(x) + \Phi(\dot{x}) \quad (2.26)$$

In the case of a power law nonlinearity given by $\Phi(x) = x^{2\eta-1}$, using Eqs. 2.18-2.20,

one can obtain the coefficients of equivalent linearization (for harmonic excitation) as,

$$\lambda = \left(\frac{\eta}{2} - 1\right)a_x^{2\eta-1} ; \nu = \left(\frac{\eta}{2}\right)a_x^{2\eta-2} \text{ and } \psi = 0 \quad (2.27)$$

and for random excitation, using Eqs. 2.22-2.24,

$$\lambda = 0; \nu = \sigma_x^{2\eta} \prod_{k=1}^{\eta} (2\eta - (2k - 1)) \text{ and } \psi = 0 \quad (2.28)$$

The range of validity of this equivalent linearizations is discussed in the next chapter in the context of TLCDs.

2.5 Concluding Remarks

In this chapter, a sloshing-slamming (S^2) damper analogy of TLD is presented. This analogy presents insights into the underlying physics of the problem and reproduces the dynamic features of TLDs at both low and high amplitudes of excitation. At low amplitudes, the S^2 damper model serves as a conventional linear sloshing damper. At higher amplitudes, the model accounts for the convection of periodically slamming lumped mass on the container wall, thus characterizing both the hardening feature and the observed increase in damping.

Next, based on the understanding of the sloshing and impact of the liquid, explicit impact characteristics are introduced into the equations of motion in order to derive a simpler mechanical model. These impact characteristics introduce the necessary nonlinearities into the system. Such mechanical models will be useful for design and analysis of TLD systems. Finally, equivalent linearization technique is used to derive linear models based on the nonlinear TLD models.